Forced and unforced variations in ocean oxygen

Matthew C. Long
Climate & Global Dynamics Laboratory
National Center for Atmospheric Research

This material is based on work supported by the National Center for Atmospheric Research, which is a major facility sponsored by the National Science Foundation under Cooperative Agreement no. 1852977.

Earth system models: internally generated variability

Range of future climate outcomes: DJF temperature trends (CCSM3, SRES-A1B)

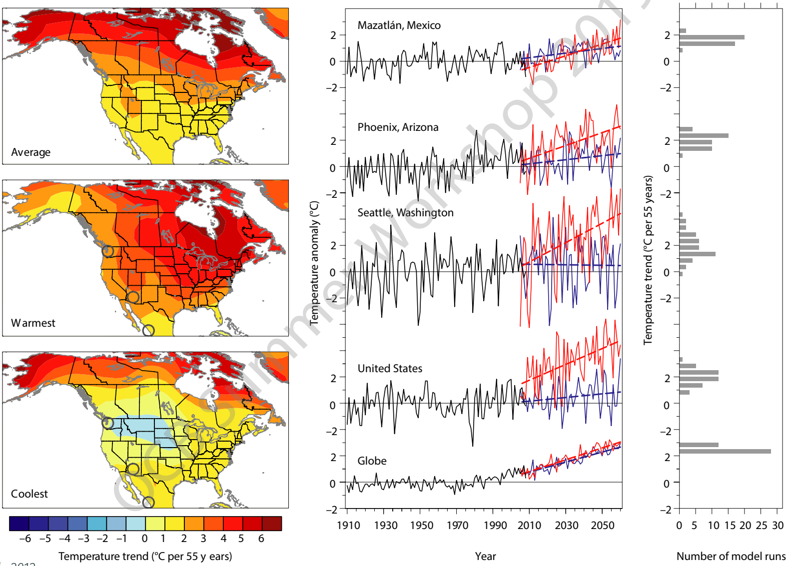

Deser et al., 2012

Physical & biological controls on interior oxygen

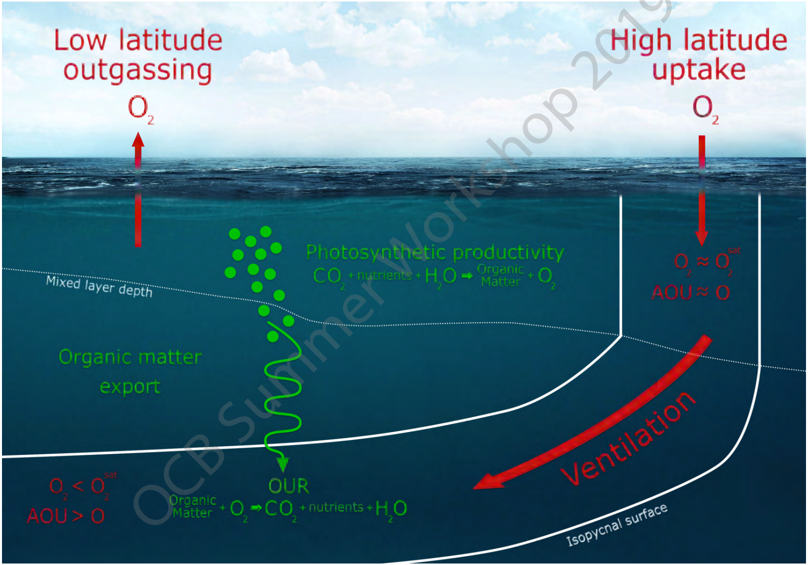

Graphic credit: M. Long and R. Johnson (NCAR)

Timescales of natural variability in thermocline O_2

Variance-weighted mean period in CESM 1850-control (400–600 m O_2)

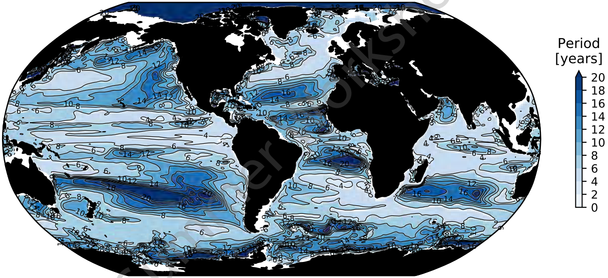

$$T_x = \sum_k V(f_k, x) \Big/ \sum_k f_k V(f_k, x)$$

Oxygen decline projected to accelerate

CESM-LE*: projected global change in O_2 & heat

* Community Earth System Model, Large Ensemble

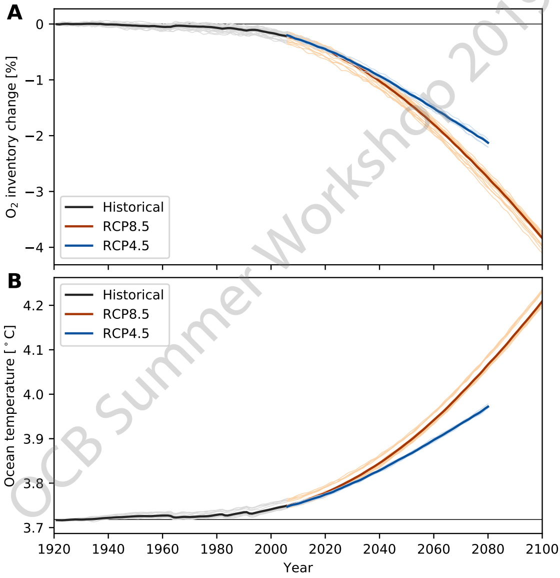

Long et al., 2019

Global zonal-mean properties: RCP8.5 & ECP8.5

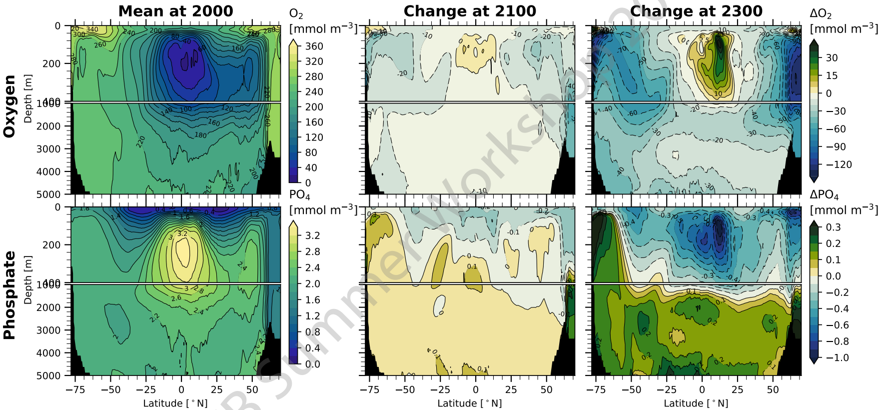

Long et al., 2019; Moore et al. 2018

CMIP5 projection: global and regional drivers of deoxygenation (2100)

AOU v. O_2^{sat} phase space: Simulated $\langle O_2 \rangle$ change ($z > -1$ km)

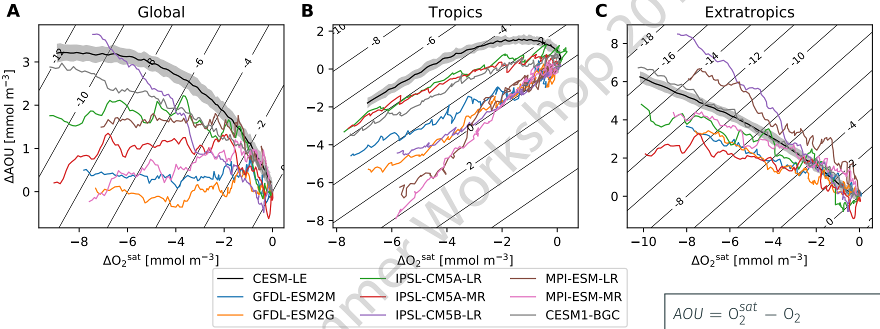

$$
\begin{aligned}
AOU &= O_2^{sat} - O_2 \\
&= f(\text{Age}, O_2\text{-utilization})
\end{aligned}
$$

- Tropics: warming compensated by reduced *AOU*;
- Extra-tropics: reinforcing *AOU* and solubility change;
- Cancelation between tropical & extra-tropical ΔAOU :
  global O_2 decline dominated by solubility effect.

Long et al., 2019

Oxygen declines related to ocean heat content anomaly

O_2^{sat} v. heat: Simulated $\langle O_2 \rangle$ change $(z > -1\ \text{km})$

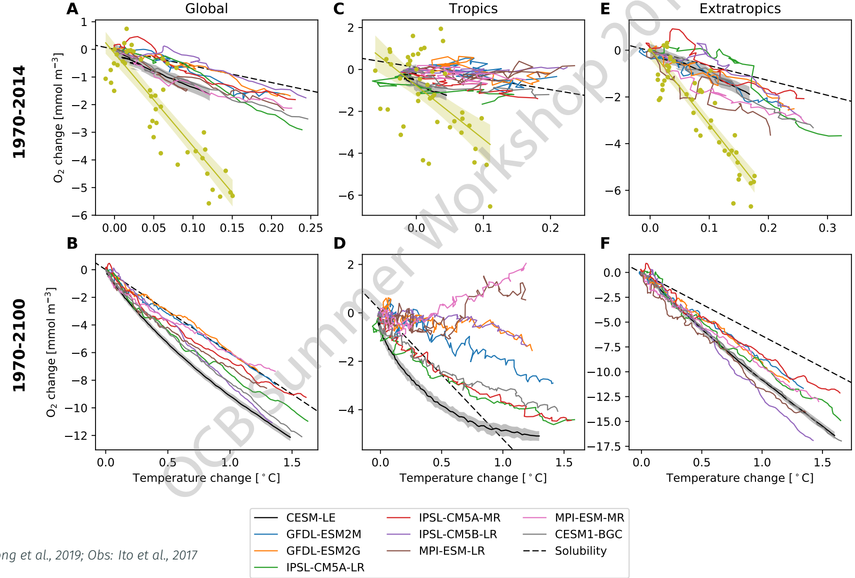

Long et al., 2019; Obs: Ito et al., 2017

Variance-weighted mean period in CESM 1850-control (400–600 m O_2)

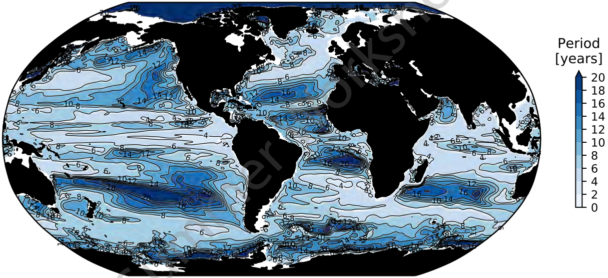

$$T_x = \sum_k V(f_k, x) / \sum_k f_k V(f_k, x)$$

Superposition of forced signal and internal variability: Total

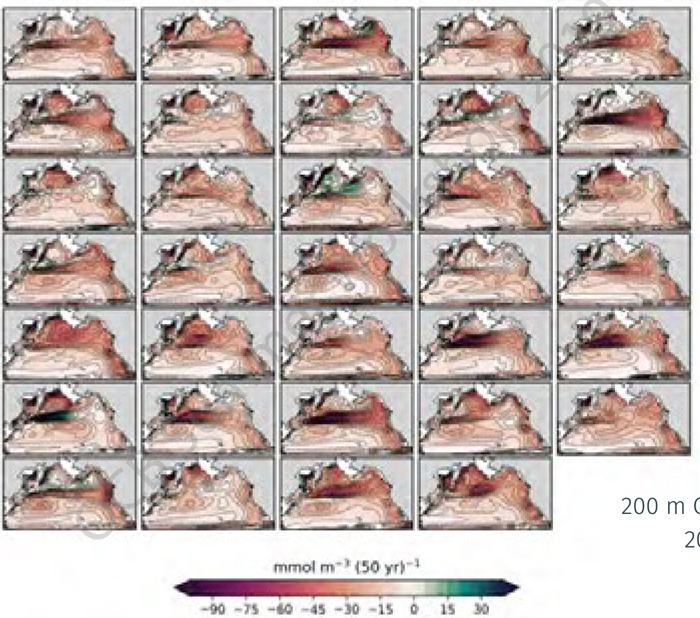

200 m O_2 trends
2006–2055

CESM Large Ensemble: Linear trends in 200 m dissolved oxygen (2006–2055)

$$\psi_i(t,x) = \widetilde{\psi}_i(t,x) + \psi^s(t,x) \qquad \widetilde{\psi}_i(t,x) \qquad \psi^s(t,x) = \frac{1}{m}\sum_{i=1}^{m}\psi_i(t,x)$$

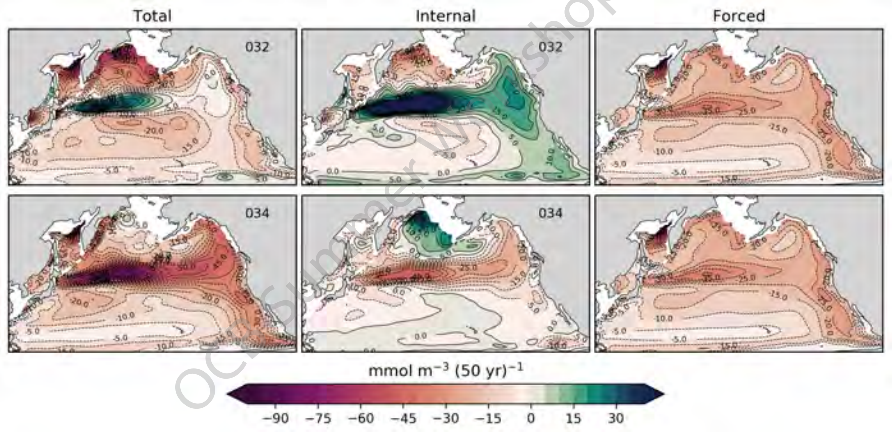

Superposition of forced signal and internal variability: Internal variability

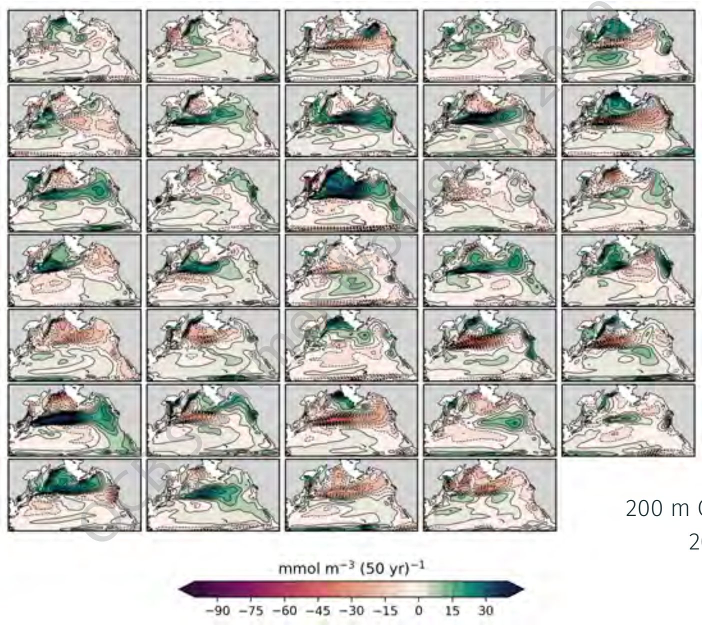

200 m O_2 trends
2006–2055

Can internal variability account for model-observations discrepancy?

Observed and simulated trends: global

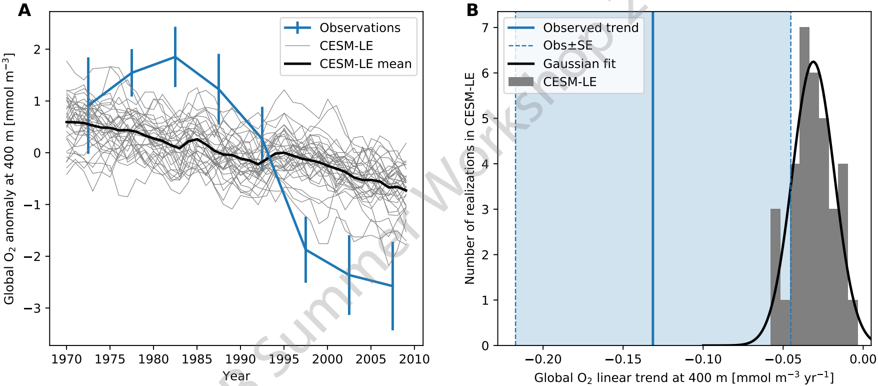

Long et al., 2019

Can internal variability account for model-observations discrepancy?

Observed and simulated trends: Subtropical North Atlantic

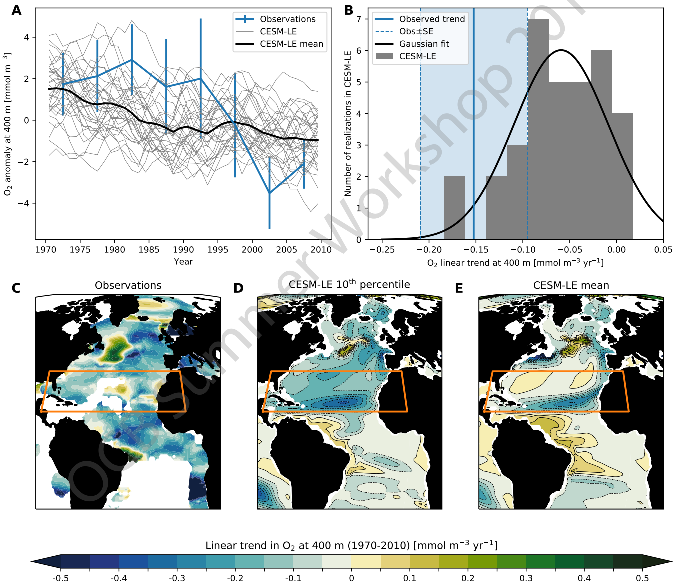

Long et al., 2019

Natural variability challenges detection and attribution

Thermocline O_2
California Current

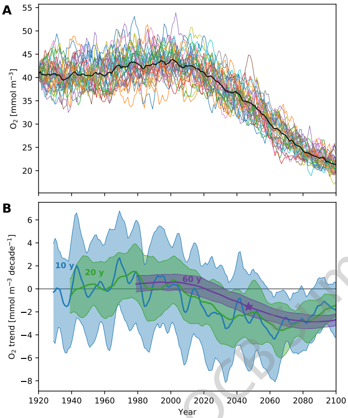

Time of emergence

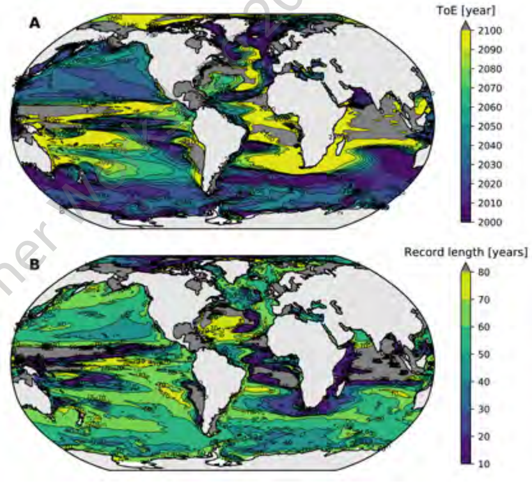

Quantifying spatial structure of $[O_2]$ variability and change

Time evolving spatial pattern

$$\psi_i(t,x) = \widetilde{\psi}_i(t,x) + \psi^s(t,x)$$

where $t = 1, \ldots, n$ and $x = 1, \ldots, p$ denote discrete time (annual means) and space (model grid points).

The forced signal

$$\psi^s(t,x) = \frac{1}{m}\sum_{i=1}^{m}\psi_i(t,x)$$

Climate anomalies

$$\psi_i'(t,x) = \psi_i(t,x) - \overline{c}(x)$$

EOF decomposition of anomalies

$$\psi_i'(t,x) = \sum_{j=1}^{q}\alpha_j^i(t)e_j^i(x)$$

Leading EOFs: Large-scale spatial patterns of variability

Natural variability

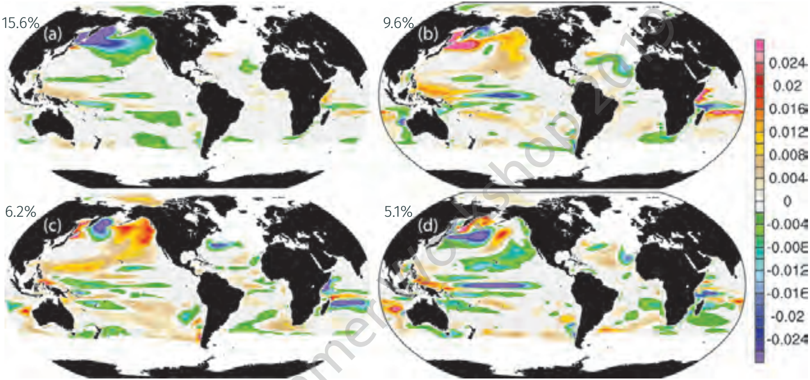

Forced signal

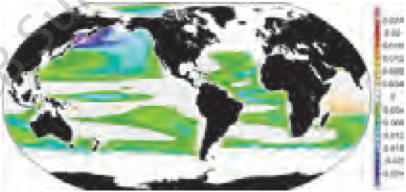

Quantifying spatial structure of $[O_2]$ variability and change

EOF decomposition of anomalies

$$\psi_i'(t,x) = \sum_{j=1}^{q} \alpha_j^i(t) e_j^i(x)$$

Projection of each ensemble member ($\psi_i'(t,x)$) onto EOF of forced signal

$$\alpha^{is}(t) = \sum_{x=1}^{p} \psi_i'(t,x) e^s(x)$$

Contribution of forced pattern to overall spatial variance

$$V_i^{is}(t) = \alpha^{is}(t)^2 \Big/ \sum_{x=1}^{p} \psi_i'(t,x)^2$$

Rising dominance of the forced signal

Percentage of total spatial variance attributable to the forced signal

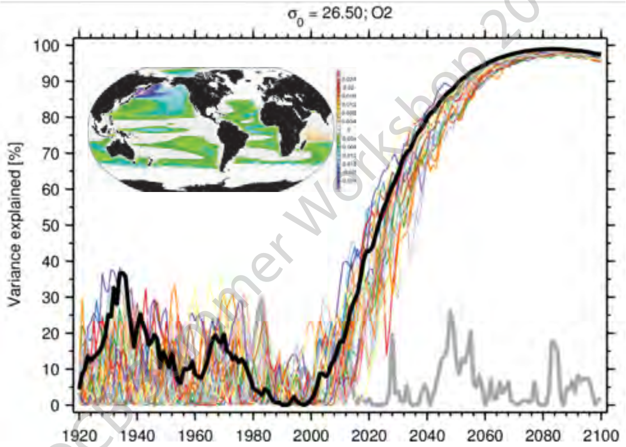

Long et al., 2016

Another forced signal: volcanic eruptions

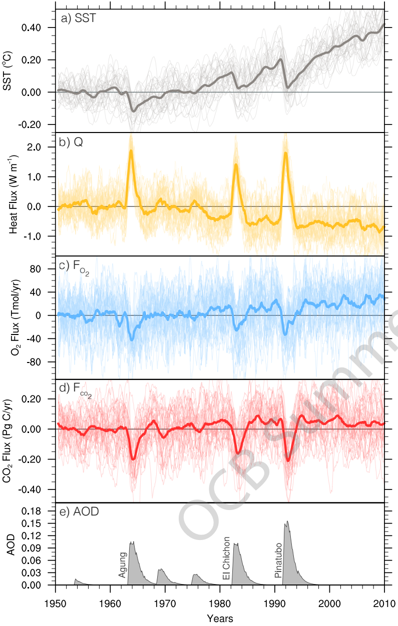

Global-mean ocean properties
CESM Large Ensemble

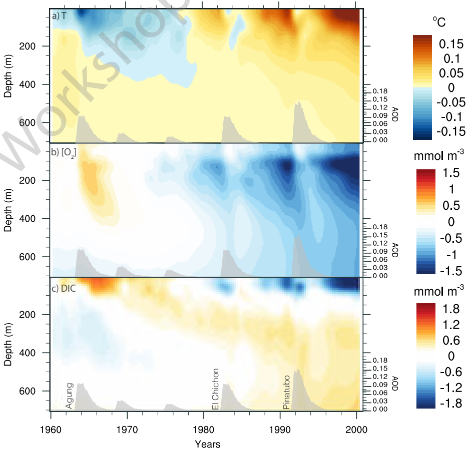

Eddebbar et al., 2019

Time-evolving distributions under changing external forcing

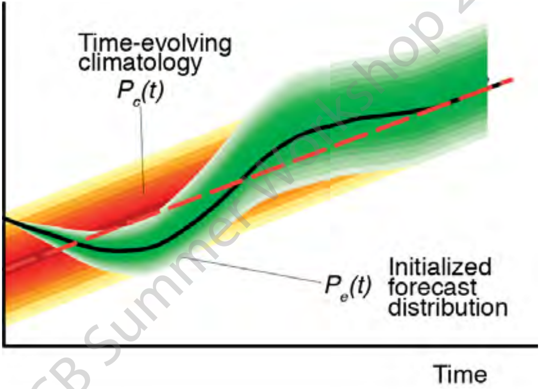

Branstator & Teng et al. 2010

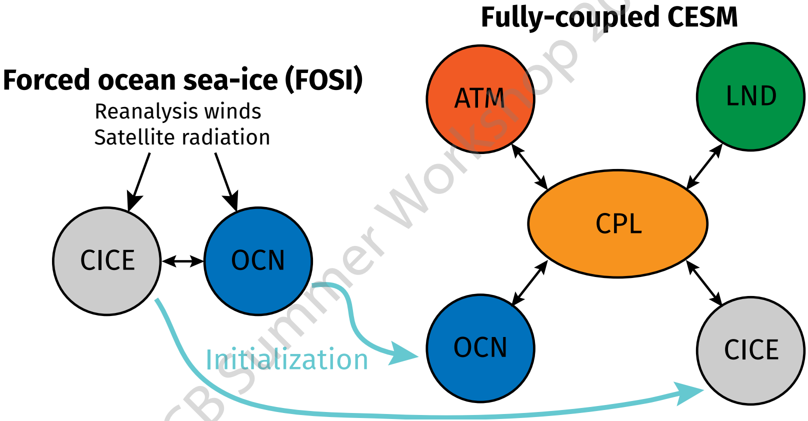
Fully-coupled CESM
Forced ocean sea-ice (FOSI)
Reanalysis winds
Satellite radiation
ATM
LND
CPL
CICE
OCN
OCN
CICE
Initialization

Skillful forecasts of upper ocean heat content on decadal timescale

Heat content anomaly, N. Atlantic Subpolar gyre ($z > -275$ m)

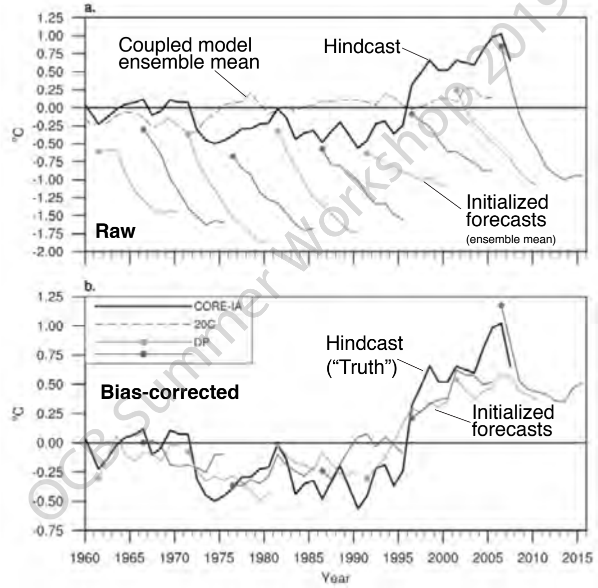

Yeager et al. 2012

Thermocline oxygen concentrations look to be highly predictable

Anomaly correlation coefficient: O_2 on $\sigma_\theta = 26.5$

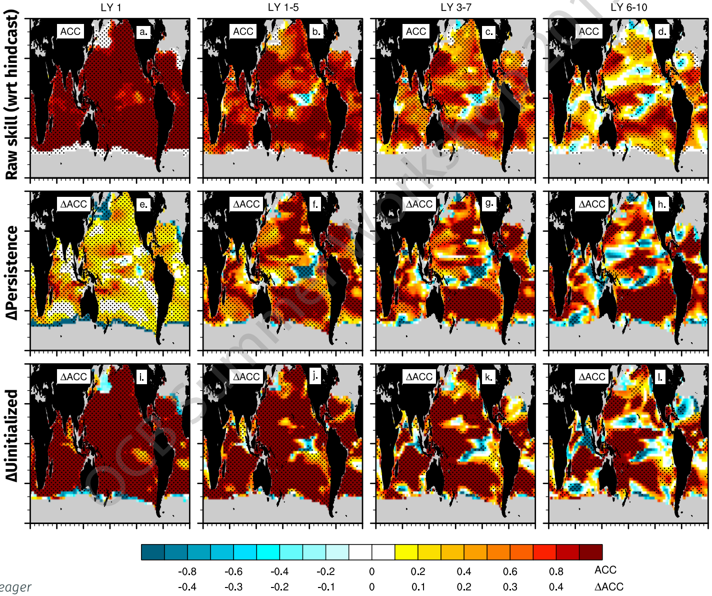

courtesy of S. Yeager

Thermocline oxygen concentrations look to be highly predictable

Anomaly correlation coefficient: Salinity on $\sigma_\theta = 26.5$

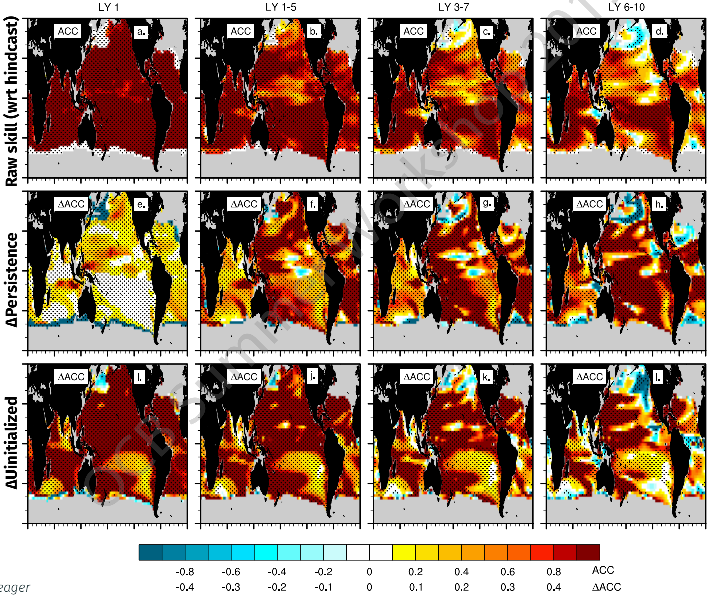

courtesy of S. Yeager

Oxygen variability at Ocean Station Papa ($\sigma_\theta = 26.5$)

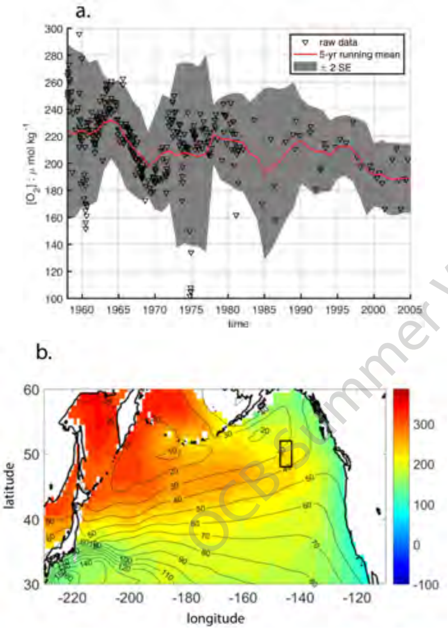

Detrended annual O_2 anomalies

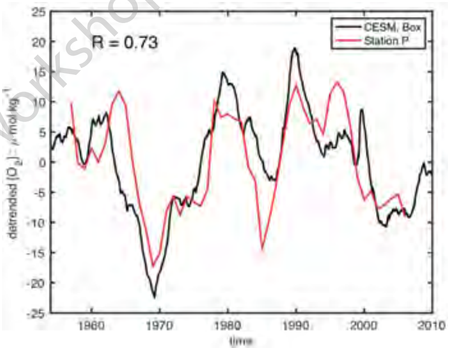

Sun & Ito, in prep

Simulated lag correlation between OSP O_2 and full field

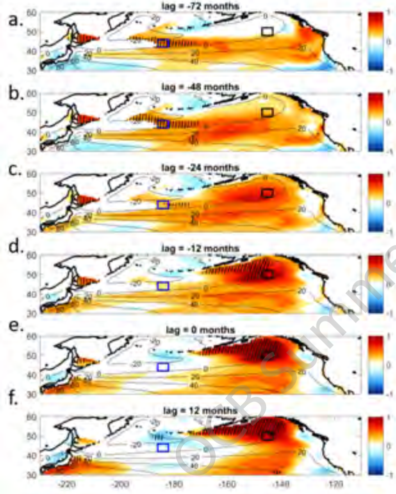

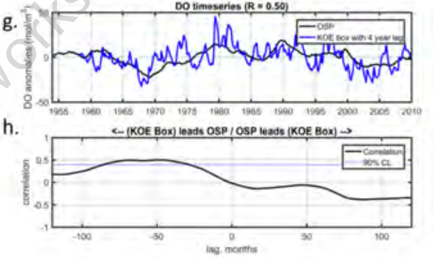

Sun & Ito, in prep

Oxygen variability at Ocean Station Papa ($\sigma_\theta = 26.5$)

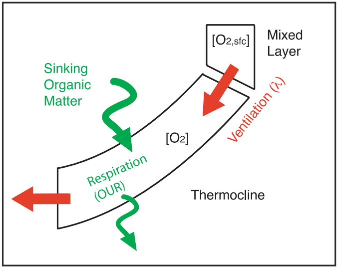

Ito & Deutsch, 2010

LIM: 3-month OSP forecast

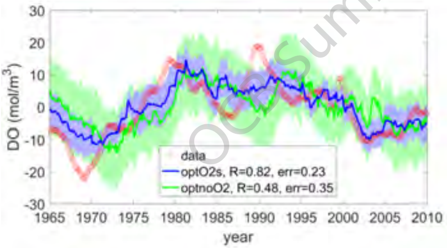

Local autoregressive (AR1) model

$$\frac{dO_2}{dt} = -\lambda O_2 + f'$$

Linear Inverse Model (LIM)

$$\frac{d\mathbf{O}_2}{dt} = \mathbf{L}\mathbf{O}_2 + \mathbf{f}'$$

$$\mathrm{C}(\tau) = \mathrm{G}(\tau)\mathrm{C}(0)$$

$$\mathrm{G}(\tau) = \exp(L \cdot \tau)$$

$$\mathrm{O}_2(t+\tau) = \mathrm{G}(\tau)\mathrm{O}_2(t)$$

$$\mathrm{L} = \tau_0^{-1} \ln\left[\mathrm{C}(\tau_0)\mathrm{C}(0)^{-1}\right]$$

Sun & Ito, in prep

Summary

- Forced changes in O_2 result from combined effects of solubility and *AOU*; models show reasonable agreement on changes at high-latitudes, but weak consensus in the tropics.
- Models underestimate *AOU*-driven deoxygenation in the upper ocean; it is unlikely that internal variability can explain this discrepancy.
- Natural variability challenges definitive attribution of O_2 trends.
- Capabilities are emerging that enable predicting O_2 on seasonal to interannual timescales.

Acknowledgements

- Eddebbar, Y. A., K. B. Rodgers, M. C. Long, A. C. Subramanian, S.-P. Xie, and R. F. Keeling (2019), El Niño–Like Physical and Biogeochemical Ocean Response to Tropical Eruptions, *J. Climate*, *32*(9), 2627–2649, 10.1175/jcli-d-18-0458.1.

- Eddebbar, Y. A., M. C. Long, L. Resplandy, C. Rödenbeck, K. B. Rodgers, M. Manizza, and R. F. Keeling (2017), Impacts of enso on air-sea oxygen exchange: Observations and mechanisms, *Global Biogeochemical Cycles*, *31*(5), 901–921, 10.1002/2017gb005630.

- Ito, T., S. Minobe, M. C. Long, and C. Deutsch (2017), Upper Ocean O_2 trends: 1958-2015, *Geophy. Res. Lett.*, 10.1002/2017GL073613.

- Long, M. C., C. A. Deutsch, and T. Ito (2016), Finding forced trends in oceanic oxygen, *Global Biogeochem. Cycles*, *30*, 10.1002/2015GB005310.

- Long, M. C., T. Ito, and C. Deutsch (2019), Oxygen projections for the future, in *Ocean deoxygenation: everyone's problem. Causes, impacts, consequences and solutions.*, edited by D. Laffoley and J. Baxter, IUCN, Gland, Switzerland, in press.

- Moore, J. K., W. Fu, F. Primeau, G. L. Britten, K. Lindsay, M. C. Long, S. C.Doney, N. Mahowald, F. Hoffman, and J. T. Randerson (2018), Sustained climate warming drives declining marine biological productivity, *Science*, *359*(6380), 1139–1143, 10.1126/science.aao6379.

- Yeager, S. G., G. Danabasoglu, N. Rosenbloom, W. Strand, S. Bates, G. Meehl, A. Karspeck, K. Lindsay, M. C. Long, H. Teng, and et al. (2018), Predicting near-term changes in the earth system: A large ensemble of initialized decadal prediction simulations using the Community Earth System Model, *Bull. Amer. Meteor. Soc.*, 10.1175/bams-d-17-0098.1.

Questions?

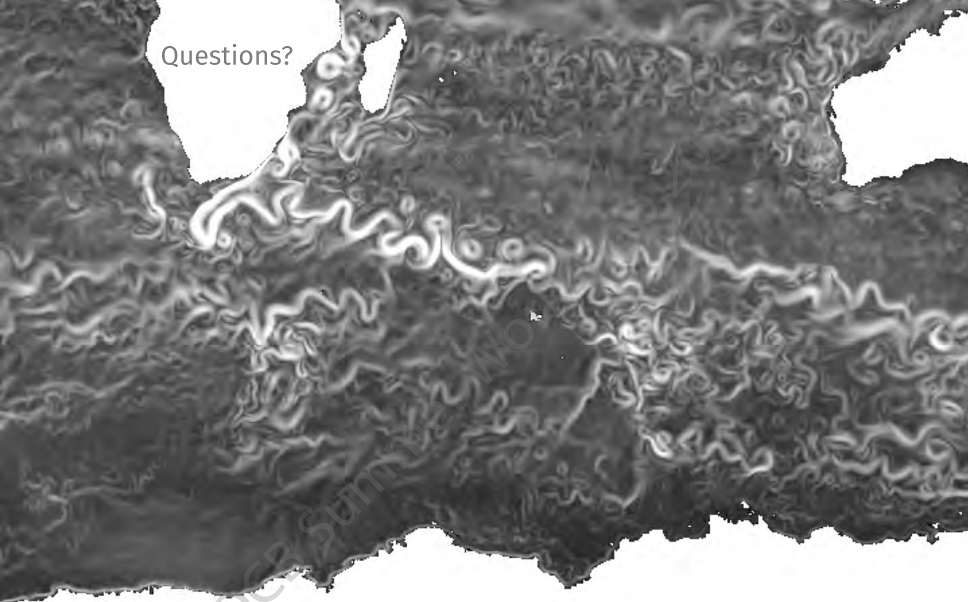

Matthew Long
Climate & Global Dynamics Laboratory
National Center for Atmospheric Research
mclong@ucar.edu

A persistent bias in Earth system models: Extensive OMZs

Thermocline (400–600 m) O_2 distributions

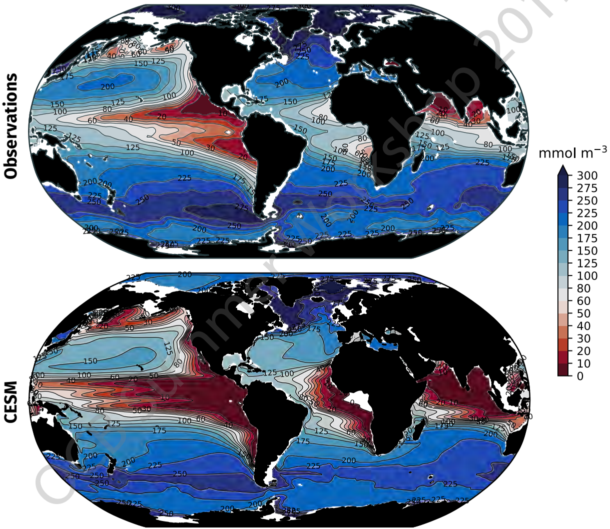

Simulated variability is weak

Simulated APO (mostly O_2) fluxes versus atmospheric inversion estimates

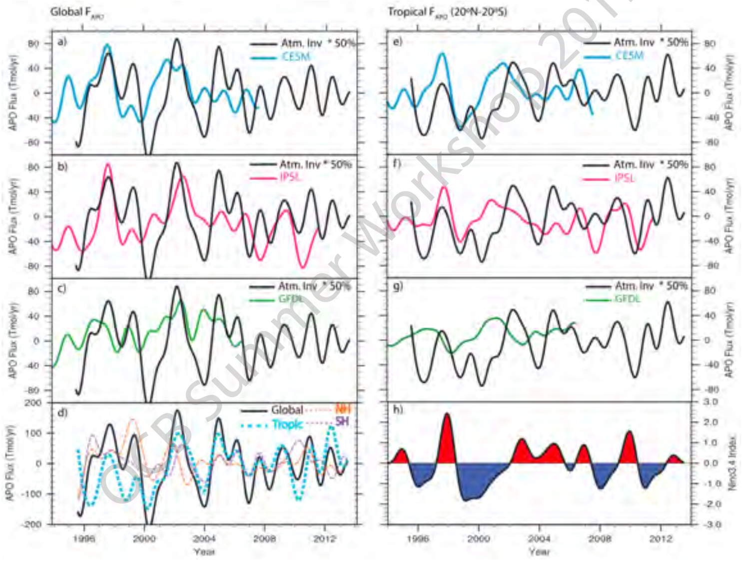

Eddebbar et al., 2017

CalCOFI dissolved oxygen is skillfully predicted

Thermocline O_2 in CalCOFI region

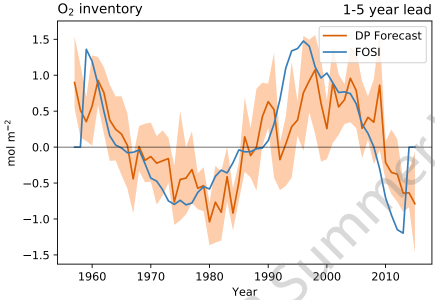

Thermocline O_2 tendency

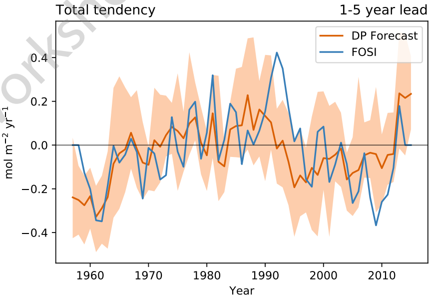

What mechanisms provide predictability for O_2?

Mean vertical gradients

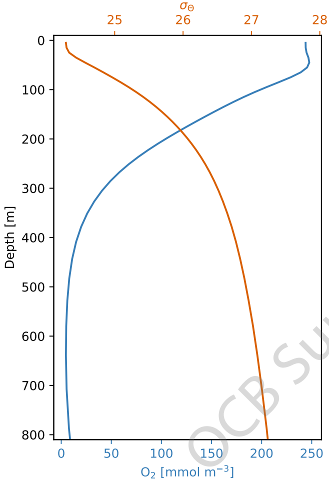

"Heave"

$$O_2^{heave} = \left(\frac{\partial \overline{O_2}}{\partial z}\right)\left(\frac{\partial \overline{\rho_\theta}}{\partial z}\right)^{-1} \rho'_\theta$$

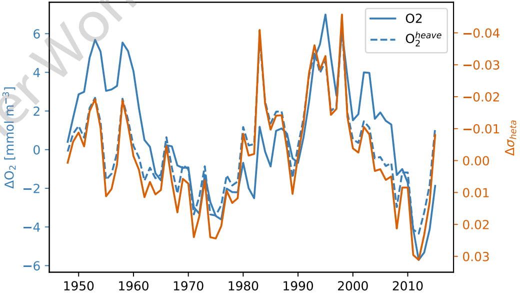

East-west difference in anomaly generation mechanism

"Ventilation regime"

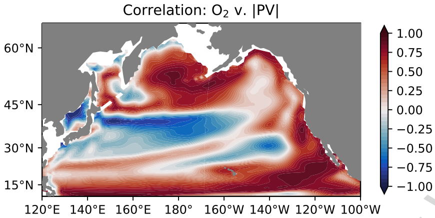

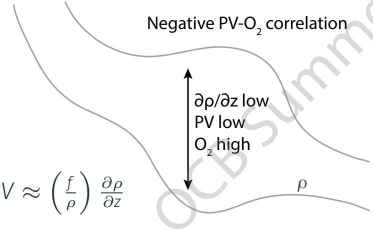

$$PV \approx \left(\frac{f}{\rho}\right)\frac{\partial \rho}{\partial z}$$

"Heave regime"

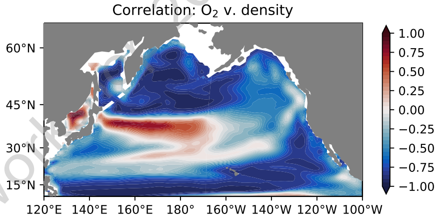

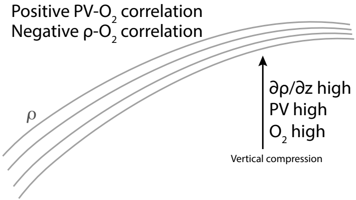

CESM-LE projection: global-mean drivers of deoxygenation

O_2 change at 2100

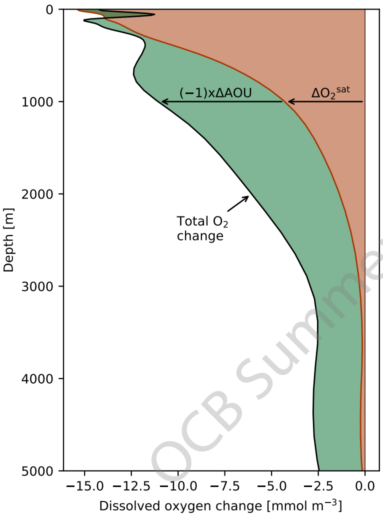

$$\Delta O_2 = \Delta O_2^{sat} - \Delta AOU$$

- Warming declines with depth;
- Surface *AOU* reduction: closer to equilibrium;
- Deep deoxygenation is *AOU*-dominated.

Long et al., 2019

Suboxic and hypoxic volumes projected to increase

Simulated change in oxygen deficient zones

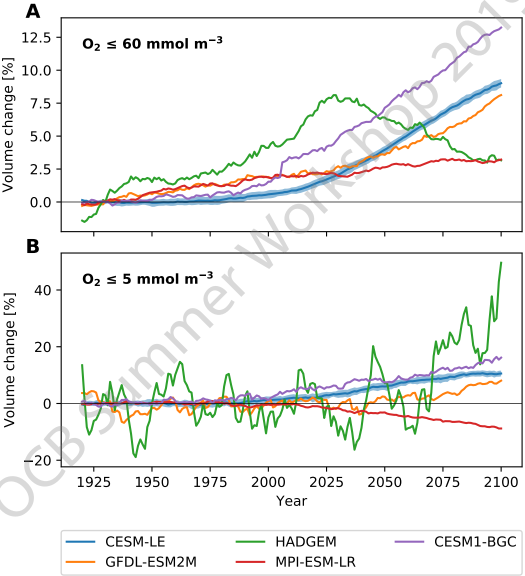

Long et al., 2019

Imprint of volcanic eruptions on ocean biogeochemistry

Response to Pinatubo (CESM-LE)

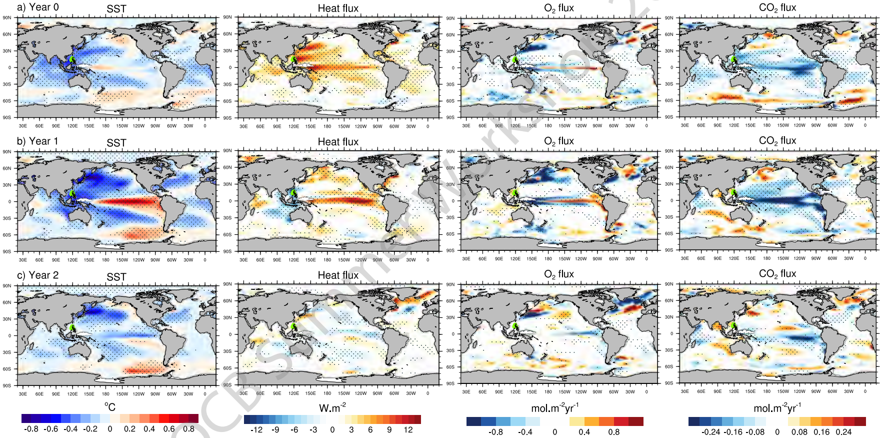

Eddebbar et al., 2019

Model resolution determines ventilation dynamics

Simulated zonal velocity at 1000 m

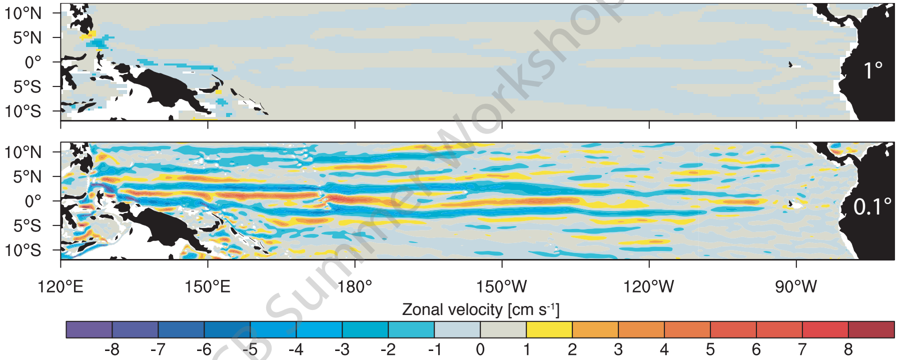

O_2 anomalies in the California Current

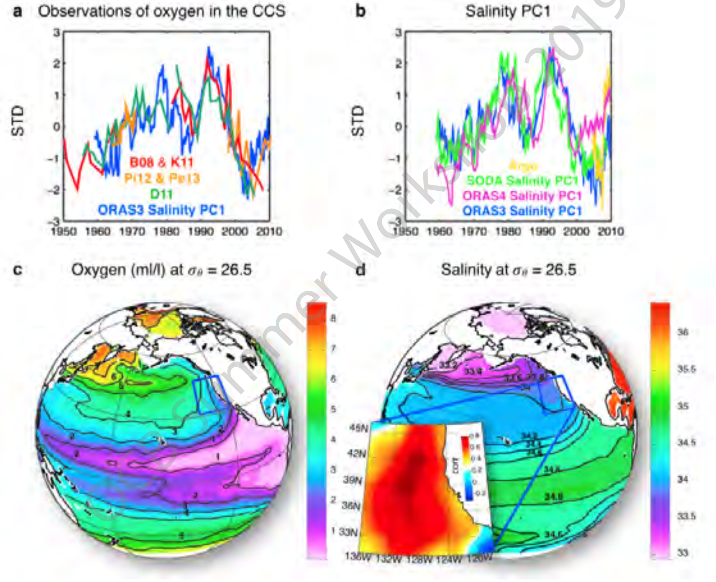

Pozo Buil & Di Lorenzo, 2017

O_2 anomalies in the California Current

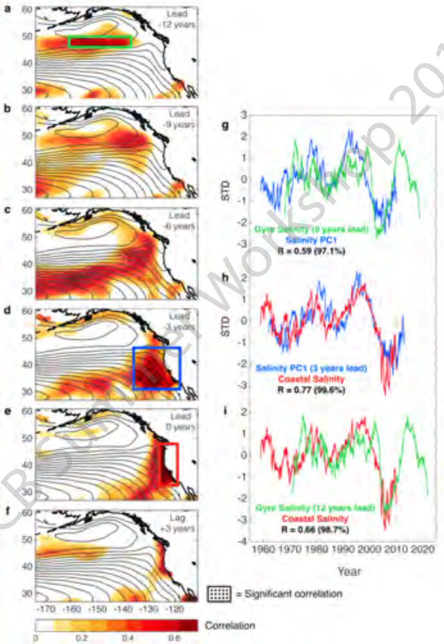

Pozo Buil & Di Lorenzo, 2017

Reinforcing drivers at high-latitudes; compensation in tropics

Simulated change in zonal-mean O_2

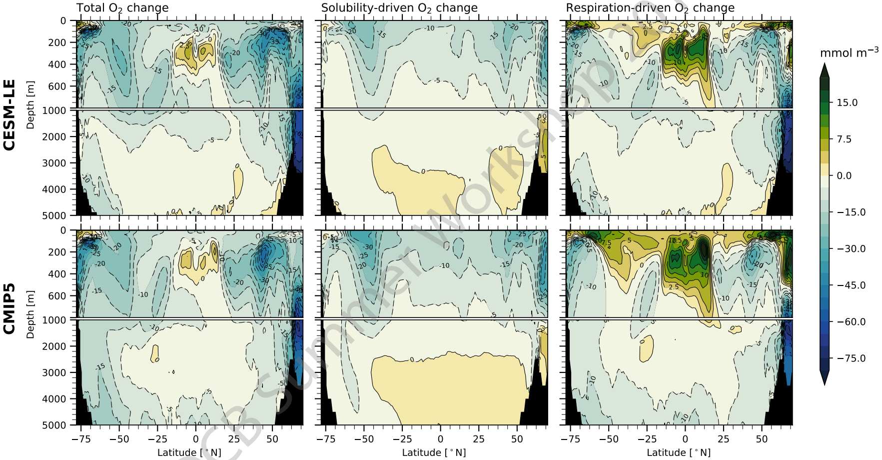

Long et al., 2019